An optical modulator based on a single strongly coupled quantum dot - cavity system in a p-i-n junction

Dirk Englund[1,2], Andrei Faraon[1], Arka Majumdar[1], Nick Stoltz[3], Pierre Petroff[3] & Jelena Vučković[1]

[1]*Department of Electrical Engineering, Stanford University, Stanford CA 94305;*
[2]*Department of Physics, Harvard University, Cambridge MA 02138;*
[3]*Dept. of Electrical and Computer Engineering, University of California, Santa Barbara, CA 93106*

Abstract: We demonstrate an optical modulator based on a single quantum dot strongly coupled to a photonic crystal cavity. A vertical p-i-n junction is used to tune the quantum dot and thereby modulate the cavity transmission, with a measured instrument-limited response time of 13 ns. A modulator based on a single quantum dot promises operation at high bandwidth and low power.

OCIS codes: (130.0130) Integrated optics; (130.3120) Integrated optics devices; (270.0270) Quantum Optics; (270.5580) Quantum electrodynamics; (23.02300) Optical devices; (230.5750) Resonators; (250.0250) Optoelectronics; (250.5300) Photonic integrated circuits

References and links

1. D. A. B. Miller, "Device Requirements for Optical Interconnects to Silicon Chips," Proc. IEEE **97**, 1166 – 1185 (2009).
2. J. Meindl, "Interconnect opportunities for gigascale integration," Micro. IEEE **23**(3), 28–35 (2003).
3. M. Lipson, "Guiding, modulating, and emitting light on Silicon-challenges and opportunities," J. Lightwave Technol. **23**(12), 4222–4238 (2005).
4. Y. Chang and L. A. Coldren, "Efficient, High-Data-Rate, Tapered Oxide-Aperture Vertical-Cavity Surface-Emitting Lasers," IEEE J. Quantum Electron. **15**(3), 1–12 (2009).
5. D. Englund, H. Altug, B. Ellis, and J. Vuckovic, "Ultrafast Photonic Crystal Lasers," Laser Photon. Rev. **2**, 1863–8880 (2008).
6. L. Chrostowski, X. Zhao, and C. Chang-Hasnain, "Microwave performance of optically injection-locked VCSELs," IEEE Trans. Microwave Theory Tech. **54**(2), 788–796 (Feb. 2006).
7. Q. Xu, B. Schmidt, S. Pradhan, and M. Lipson, "Micrometre-scale silicon electro-optic modulator," Nature **435**(7040), 325–327 (2005).
8. H.-W. Chen, Y. hao Kuo, and J. E. Bowers, "High speed hybrid silicon evanescent Mach-Zehnder modulator and switch," Opt. Express **16**(25), 20571–20576 (2008).
9. Y. Vlasov, W. M. J. Green, and F. Xia, "High-throughput silicon nanophotonic wavelength-insensitive switch for on-chip optical networks," Nat. Photon **2**, 242 – 246 (2008).
10. Q. Xu, D. Fattal, and R. G. Beausoleil, "Silicon microring resonators with 1.5μm radius," Opt. Express **16**(6), 4309–4315 (2008).
11. T. Yoshimatsu, S. Kodama, K. Yoshino, and H. Ito, "100-gb/s error-free wavelength conversion with a monolithic optical gate integrating a photodiode and electroabsorption modulator," IEEE Photon. Technol. Lett. **17**(11), 2367–2369 (2005).
12. J. Roth, O. Fidaner, E. Edwards, R. Schaevitz, Y.-H. Kuo, N. Herman, T. Kamins, J. Harris, and D. Miller, "C-band side-entry ge quantum-well electroabsorption modulator on SOIi operating at 1 V swing," Electron Lett. **44**(1), 49–50 (2008).
13. A. Agarwal and J. H. Lang, *Foundations of Analog and Digital Electronic Circuits* (Morgan Kaufmann, 2005).
14. D. Englund, A. Faraon, I. Fushman, N. Stoltz, P. Petroff, and J. Vučković, "Controlling cavity reflectivity with a single quantum dot," Nature **450**(6), 857–61 (2007).

#114379 - $15.00 USD Received 16 Jul 2009; revised 21 Sep 2009; accepted 24 Sep 2009; published 1 Oct 2009

15. K. Srinivasan and O. Painter, "Linear and nonlinear optical spectroscopy of a strongly coupled microdisk-quantum dot system," Nature **450**, 862–865 (2007).
16. D. Englund, D. Fattal, E. Waks, G. Solomon, B. Zhang, T. Nakaoka, Y. Arakawa, Y. Yamamoto, and J. Vučković, "Controlling the Spontaneous Emission Rate of Single Quantum Dots in a Two-Dimensional Photonic Crystal," Phys. Rev. Lett. **95**, 013,904 (2005).
17. Y. Akahane, T. Asano, B.-S. Song, and S. Noda, "High-Q photonic nanocavity in a two-dimensional photonic crystal," Nature **425**, 944–947 (2003).
18. M. Toishi, D. Englund, A. Faraon, and J. Vučković, "High-brightness single photon source from a quantum dot in a directional-emission nanocavity," Opt. Express **17**(17), 14618–14626 (2009).
19. H. Park, S. Kim, S. Kwon, Y. Ju, J. Yang, J. Baek, S. Kim, and Y. Lee, "Electrically driven single-cell photonic crystal laser," Science **305**, p.1444–7 (2004).
20. A. Laucht, F. Hofbauer, N. Hauke, J. Angele, S. Stobbe, M. Kaniber, G. Bohm, P. Lodahl, M.-C. Amann, and J. J. Finley, "Electrical control of spontaneous emission and strong coupling for a single quantum dot," New J. Phys. **11**(2), 023,034 (11pp) (2009).
21. D. Englund, B. Ellis, E. Edwards, T. Sarmiento, J. S. Harris, D. A. B. Miller, and J. Vuckovic, "Electrically controlled modulation in a photonic crystal nanocavity," Opt. Express **17**(18), 15,409–15,419 (2009).
22. M. B. Yairi, H. V. Demir, P. B. Atanackovic, and D. A. B. Miller, "Large-Signal Response of p-i-n Photodetectors Using Short Pulses With Small Spot Sizes," IEEE J. Quantum Electron. **40**(2), 143–151 (2004).
23. D. Englund, A. Faraon, B. Zhang, Y. Yamamoto, and J. Vuckovic, "Generation and transfer of single photons on a photonic crystal chip," Opt. Express **15**, 5550–8 (2007).
24. A. Faraon, I. Fushman, D. Englund, N. Stoltz, P. Petroff, and J. Vuckovic, "Dipole induced transparency in-waveguide coupled photonic crystalcavities," Opt. Express **16**(16), 12,154–12,162 (2008).
25. M. Bass, ed., *Fiber Optics Handbook* (Mc Graw - Hill, 2002).
26. A. I. Bachir, N. Durisic, B. Hebert, P. Grütter, and P. W. Wiseman, "Characterization of blinking dynamics in quantum dot ensembles using image correlation spectroscopy," J. Appl. Phys. **99**(6), 064503 (pages 7) (2006).
27. D. Englund, H. Altug, and J. Vučković, "Low-Threshold Surface-Passivated Photonic Crystal Nanocavity Laser," Appl. Phys. Lett. **91**, 071,124 (2007).
28. R. Schmidt, U. Scholz, M. Vitzethum, R. Fix, C. Metzner, P. Kailuweit, D. Reuter, A. Wieck, M. C. Hübner, S. Stufler, A. Zrenner, S. Malzer, and G. H. Döhler, "Fabrication of genuine single-quantum-dot light-emitting diodes," Appl. Phys. Lett. **88**(12), 121115 (pages 3) (2006).
29. E. Waks and J. Vučković, "Dipole induced transparency in drop-filter cavity-waveguide systems," Phys. Rev. Lett. **96**(153601) (2006).
30. A. Auffeves-Garnier, C. Simon, J. Gerard, and J.-P. Poizat, "Giant optical nonlinearity induced by a single two-level system interacting with a cavity in the Purcell regime," Phys. Rev. A **75**, 053,823 (2007).
31. X. Chen, Y.-S. Chen, Y. Zhao, W. Jiang, and R. T. Chen, "Capacitor-embedded 0.54 pJ/bit silicon-slot photonic crystal waveguide modulator," Opt. Lett. **34**(5), 602–604 (2009).
32. A. Faraon, A. Majumdar, H. Kim, P. Petroff, and J. Vuckovic, "Fast Electrical Control of a Quantum Dot Strongly Coupled to a Nano-resonator," arXiv:0906.0751v1 [quant-ph] (2009).

1. Introduction

In recent years, optical interconnects have emerged as a potential replacement for metallic interconnects to address limitations in power consumption, latency, and bandwidth[1, 2, 3]. One of the primary challenges of optical interconnects is to reduce the energy requirement, with a targeted energy-per-bit near $\sim$ 10 fJ/bit for chip-to-chip communication over the next decades [1]. While there has been steady progress in power and speed of directly modulated laser sources[4, 5, 6] and modulators with external lasers [7, 8, 9, 10, 11, 12], the 10 fJ/bit target remains extremely challenging. One approach is to dramatically miniaturize the active region. Since a capacitive modulator requires an energy-per-bit of $U = CV^2/2$, where C is the capacitance and V the swing voltage[13], the switching energy can be reduced with the size, and hence the capacitance, of the device. The smallest size may be reached with a single emitter, such as a quantum dot (QD). The absorption cross section of a single QD is too small, but it can be greatly enhanced in a nanocavity[14, 15]. In particular, we showed that a single QD strongly coupled to a photonic crystal (PC) cavity effectively controls the cavity reflection[14]. Here, we build on this result to modulate the transmission of a cavity by shifting the QD in a p-i-n junction. The voltage across the p-i-n junction is varied by optical carrier injection, but may instead be controlled with electrical contacts. We measure a modulation response time of

#114379 - $15.00 USD Received 16 Jul 2009; revised 21 Sep 2009; accepted 24 Sep 2009; published 1 Oct 2009

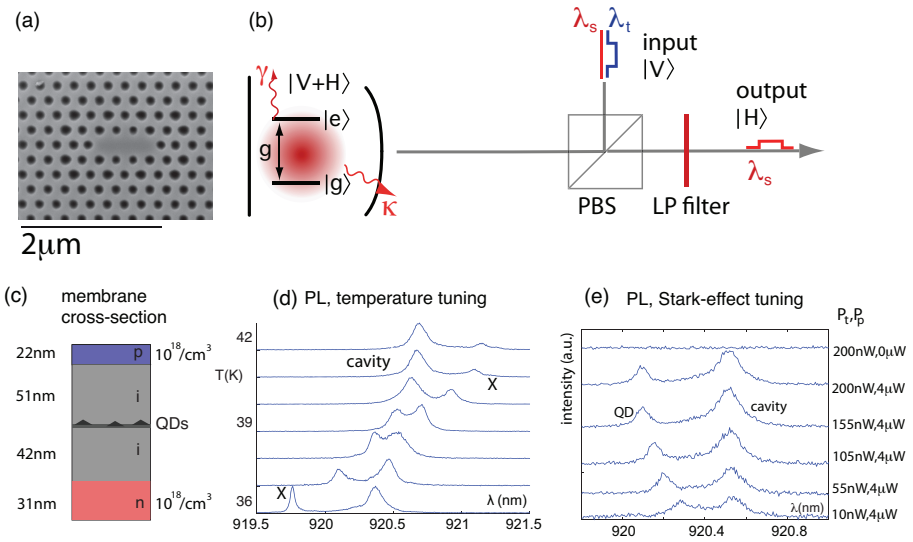

Fig. 1. (a) Scanning electron micrograph of the photonic crystal. (b) In the experiment, a signal laser (at $\lambda_s \sim 920.5$nm) and a tuning laser ($\lambda_t \sim 780$nm) are incident on the cavity at a vertical polarization ($|V\rangle$). The cavity is linearly polarized at 45° ($|V+H\rangle/\sqrt{2}$) and is backed by a distributed Bragg reflector, effectively creating a single-sided cavity. The modulated signal beam is measured in the horizontally polarized output port after a 900 nm long pass filter. (c) Illustration of the p-i-n junction integrated in the GaAs PC membrane. (d) Anticrossing observed in the PL as the QD single exciton (X) is temperature-tuned through the cavity. The QD is pumped through higher-order excited states by optical excitation at a wavelength of $\lambda_e = 873$ nm. (e) The QD blue-shifts as the power P_t of the tuning laser at 780 nm is increased while the pump laser power P_p is fixed. If the pump is turned off, the PL is dramatically reduced.

13 ns (limited by the speed of the modulation laser). Because of a residual charging effect, the modulation speed is limited to ~ 5 MHz with an energy-per-bit near 200 fJ, though it appears that bandwidths exceeding 10 GHz and energies well below 1fJ/bit are possible by electrically contacting the p-i-n junction. Our use of the QD/cavity system as a modulator suggests that the strong light/matter interaction achievable in cavity quantum electrodynamic systems could provide the basis for a new class of classical information processing devices for applications demanding high speed and low power.

2. System characterization

The sample is grown by molecular beam epitaxy. A 160-nm thick, GaAs membrane contains a central layer of self-assembled InAs QDs with a density of $\sim 50/\mu\text{m}^2$. The single exciton emission of the dots is distributed around 910-940 nm. The GaAs membrane is doped to form a vertical p-i-n diode with the QD layer in the intrinsic region (Fig. 1(c)). Both *p* and *n* regions have a doping concentration near $10^{18}/\text{cm}^3$. The photonic crystal structures are then fabricated by a combination of electron beam lithography and dry/wet etching steps[16].

The optical system considered here consists of a self-assembled InAs quantum dot (QD) coupled to a three-hole defect (L3) PC cavity (Fig. 1(a)). The cavity design is based on Ref.[17], but is modified with a set of perturbations to increase the directionality of the radiated field[18]. Since the perturbations introduce some additional photon loss, the cavity quality factor is only 6000, somewhat lower than unperturbed cavities in similar experiments[14]. The sample is cooled to 20-50 K inside a continuous-flow cryostat and analyzed in the confocal microscope

#114379 - $15.00 USD Received 16 Jul 2009; revised 21 Sep 2009; accepted 24 Sep 2009; published 1 Oct 2009

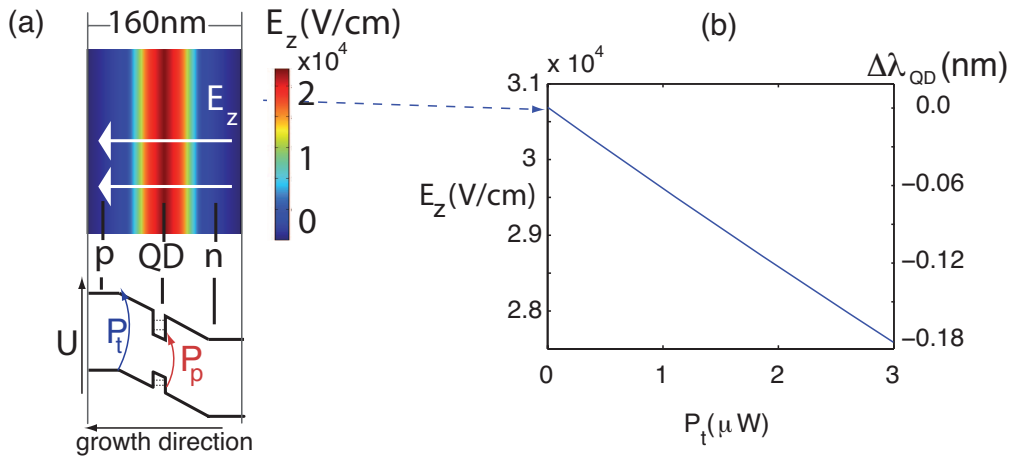

Fig. 2. Simulation of electric field dependence on the photogenerated carriers. (a) Electric field dependence across the p-i-n junction. The QDs are located near the field maximum. The tuning laser with power P_t and wavelength $\lambda_t = 780$nm creates carriers in the GaAs membrane. The pump laser (power P_p) is tuned to 860nm to create carriers only in the QDs and the QD-wetting layer. (b) Simulated electric field dependence at the center of the membrane as a function of the absorbed power P_t of the tuning laser. The QD wavelength shift is calculated from the the experimentally measured vertical Stark shift[20] and is indicated by the scale on right hand side.

setup illustrated in Fig. 1(b). As shown in the photoluminescence (PL) in Fig. 1(d), the QD- and cavity-like states anticross as the QD is thermally tuned through the cavity. The vacuum Rabi splitting of 0.16 nm exceeds the cavity linewidth (0.15 nm), indicating that the QD/cavity system is in the strong coupling regime.

2.1. Controlling the QD in a p-i-n junction

The dot is tuned in the p-i-n junction by a process that we identify as the DC Stark shift. This shift has been demonstrated previously using electrical contacts to control an electric field across the QD[19, 20, 21]. However, to facilitate testing of many devices inside the cryostat, we instead modulate the built-in DC electric field in the p-i-n junction optically, by photogenerated charge separation across the PC membrane. The charge carriers are created with a 'tuning' laser at wavelength $\lambda_t = 780$nm (frequency ω_t above the GaAs bandgap energy) and power P_t in the microwatt range. The beam is focused to $\sim 5\mu$m to cover the PC structure.

Figure 2(a) shows a simulation of the built-in electric field across the p-i-n junction. The QD layer is located near the electric field maximum of ~ 20kV/cm. In the simulation, a source term models the photogenerated carrier density by $P_t/(\hbar\omega_t V_t)$, where V_t is the volume on which the tuning laser is incident. The accumulation of photogenerated carriers changes the electric field across the QDs in the sample growth direction, as shown in Fig. 2(b). The simulated electric field[1] is used to calculate the expected Stark shift on the QD, based on data from Ref.[20], as is shown in the scale on the right hand side of Fig. 2(b). From the model, we therefore expect a change in the QD wavelength of $\Delta\lambda_{QD} \sim 0.1$ nm at a tuning laser power of $\sim 1\mu$W.

To characterize the electric field across the p-i-n junction and its effect on the QD, we plot in Fig. 1(e) the photoluminescence (PL) when the tuning laser power P_t is increased from zero

[1]In the simulation, the tuning laser spot is assumed to be Gaussian with a FWHM of 5 μm; doping concentrations in the membrane are given in Fig. 1(c); the carrier generation, diffusion, and drift are solved simultaneously using the Comsol software package.

#114379 - $15.00 USD Received 16 Jul 2009; revised 21 Sep 2009; accepted 24 Sep 2009; published 1 Oct 2009

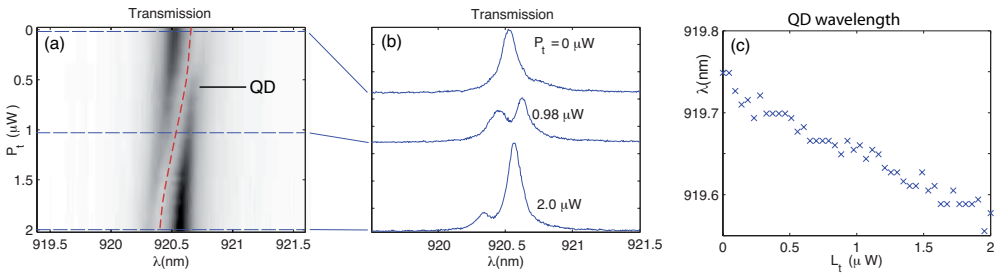

Fig. 3. (a) The broad-band transmission shows the QD tuning through the cavity resonance as the tuning laser power P_t is increased. (b) Detail of broad-band reflectivity. (c) QD wavelength obtained from the local minimum corresponding to the QD position in (a).

to 200 nW. We simultaneously create carriers in the QD in the PC with a pump laser at 860 nm at a power of $P_p = 4\mu$W, measured before the objective lens. The pump laser is not absorbed in the bulk GaAs since its frequency is below the bandgap, and therefore the pump laser is not expected to significantly affect the bias voltage across the QD. The QD/cavity system is initially tuned on resonance by temperature, so we observe two nearly equally intense polariton modes (bottom plot in Fig. 1(e)). When P_t is raised, the system detunes as the QD transition frequency is blue-shifted. We note that the tuning laser itself does not appreciably contribute to the QD photoluminescence: when the pump laser is turned off, the PL vanishes.

3. QD-controlled cavity transmission

We describe now how the cavity transmission is measured and controlled by the QD. As illustrated in Fig. 1(b), an external, vertically polarized (V) probe beam is coupled into the cavity, which itself is linearly polarized at 45° ($|V+H\rangle/\sqrt{2}$). The reflection is measured in the horizontal polarization ($|H\rangle$) to reduce the uncoupled background field[14]. This reflectivity measurement may be equivalently viewed as a cavity transmission measurement from the vertical ($|V\rangle$) to horizontal ($|H\rangle$) polarization.

The transmission function is first probed using a broadband light source, as plotted in Fig. 3(a). The graph shows the QD-induced transmission dip as the dot is scanned across the cavity resonance by raising P_t from 0 to 2 μW. The spectra in Fig. 3(b) show the strong contrast in the transmission spectrum as the QD is tuned from the red-detuned starting point ($P_t = 0$) onto resonance with the cavity ($P_t \sim 1\mu$W) to the blue-detuned condition at $P_t = 2\mu$W. The dashed line in Fig. 3(a) is a guide to the eye for the QD transition with tuning power; in Fig. 3(c), we plot the actual QD wavelength which is extracted from a fit to the transmission spectra. Comparing these observations with our theoretical model, we find good agreement: at a tuning power of 2μW, the QD shift is $\Delta\lambda_{QD} \sim -0.16$ nm, close to the calculated value of -0.12 nm. We do not expect perfect agreement since the carrier distribution in the model is only a rough approximation, but we find that the model adequately describes the tuning behavior of the QD.

Although the broad-band transmission shows the electric field dependence of the QD single exciton wavelength, the spectral features are limited by the resolution of the spectrometer ($\sim$ 0.03 nm). To increase the resolution, we replace the broad-band source with a narrow-band laser that is tuned near the QD transition. Figure 4(a) shows the transmission of the QD/cavity system when the narrow (linewidth < 10 MHz) probe laser is coupled into the cavity and the QD is then tuned across the cavity resonance by the electric field. A weak pump laser ($\lambda = 860$ nm with $P_p = 4\mu$W) simultaneously excites the QD so that the QD single-exciton wavelength is visible in the figure. In Fig. 4(b), we plot the observed probe transmission as the QD is tuned

#114379 - $15.00 USD Received 16 Jul 2009; revised 21 Sep 2009; accepted 24 Sep 2009; published 1 Oct 2009

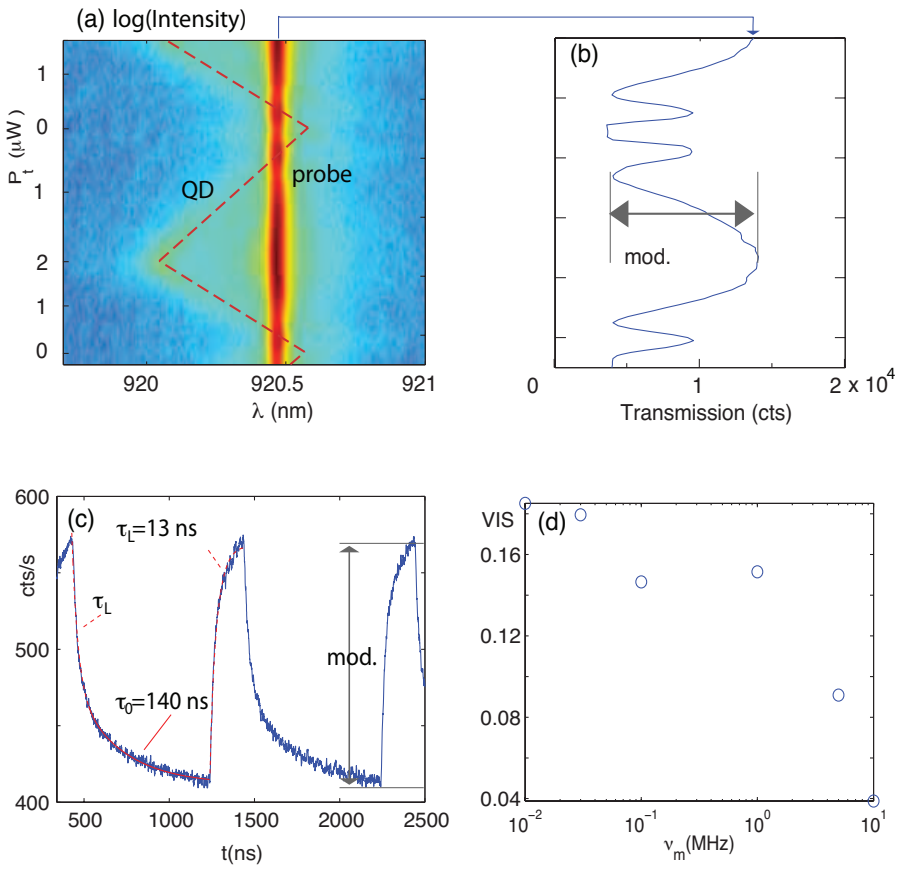

Fig. 4. Modulating the cavity transmission by DC Stark shift of the QD. (a) The cavity transmission is probed by a narrow laser on resonance with the cavity as the dot is tuned across the cavity resonance. Pump laser power is 4μW; P_t is varied between 0 and 2μW; the probe laser power is ~ 2 nW. (b) Transmission corresponding to (a) as the QD is tuned through the cavity. (c) Detector count rate I from the cavity transmission at a modulation frequency of $\nu_m = 1$ MHz. A double-exponential fit gives the response times $\tau_L \approx 13$ ns and $\tau_0 \approx 140$ ns. (d) Visibility (VIS) of the transmission as the modulation frequency ν_m is increased.

#114379 - $15.00 USD Received 16 Jul 2009; revised 21 Sep 2009; accepted 24 Sep 2009; published 1 Oct 2009

through the cavity. Large contrast is observed as the QD is tuned through the cavity resonance. We note that the PL from the QD is negligible in the transmission — it is 160 times weaker than the intensity of the transmitted probe at maximum.

To measure the modulation speed, the narrow probe laser is tuned to the cavity resonance while the QD is shifted between the positions corresponding to the highest and lowest transmission values in Fig. 4(b). The tuning laser is modulated with a square wave envelope between 0.5μW and 2μW at a frequency ν_m. The time-resolved transmission is then measured on an avalanche photodiode. Figure 4(c) plots the measured photodiode count rate I for a modulation speed of $\nu_m = 1$ MHz. To better resolve the time-dependent features, we used a duty cycle that keeps the QD detuned from the cavity (high transmission) for 20% of each period. Two time-scales are responsible for the time domain data show in Fig. 4(c): a response time of $\tau_L \sim 13$ns corresponding to the modulation bandwidth of the tuning laser; and a slow relaxation time of $\tau_0 \sim 140$ ns. Because of the long relaxation time, we expect a high frequency cutoff near 7 MHz; this is confirmed by a measurement of the modulation visibility VIS=$(\max(I) - \min(I))/(\max(I) + \min(I))$ with frequency, which indicated a cut-off near 5 MHz (Fig. 4(d)). τ_0 is much longer than the approximate RC response time of the capacitive layer (~ 10 ns) and the diffusion time of the carriers [22]. We speculate that trapped charges, potentially in nearby quantum dots, contribute to the screening of the field across the p-i-n junction, but the exact mechanism is presently not clear. The visibility in the pulsed measurement is considerably lower than the values obtained under slow tuning (for instance, the visibility in Fig. 3(b) reaches VIS~ 0.61 and a corresponding modulation depth of ~ 6.3dB). A major factor in the reduced visibility is drifting of the alignment of the tuning and probe lasers, which made it difficult to maintain the optimal transmission contrast during the data acquisition; in the future, the stability could be improved in waveguide-coupled designs[23, 24]. We also note that we did not observe frequency broadening of the transmitted field and expect chirp to be small, as in other electrorefractive modulators[25].

The modulation speed of the device is determined by two factors: the electrical bandwidth corresponding to the contacts, and the inherent 'optical bandwidth' corresponding to the response of the coupled QD-cavity system. As mentioned above, the electrical bandwidth appears limited in the present device by trapped charge states which may be reduced by improved material growth and processing[26, 27]. The bandwidth is additionally limited by the contact's RC time constant, which, however, could be as low as 10 ps[28]. Meanwhile, the optical bandwidth is limited by the response time of the coupled QD-cavity system. In the weak-coupling regime, this limit corresponds to the scattering rate of the QD[29, 30], given by the modified QD spontaneous emission rate rate $F\Gamma_0$, where F denotes the Purcell factor and Γ_0 the natural decay rate of the QD. From lifetime measurements of uncoupled QDs, we estimate $\Gamma_0 \sim 1$ GHz. In the strong coupling regime, the QD-cavity coupling rate g exceeds the cavity field and QD dipole decay rates, $g > \kappa, \Gamma_0/2$. The strongly coupled system's response rate is then limited by the cavity intensity decay rate 2κ, corresponding to $\kappa/\pi \sim 50$ GHz. In the present device, the optical bandwidth is clearly much faster than the electrical bandwidth and therefore does not limit the overall modulation speed.

To estimate the energy-per-bit, we consider the average applied power on the order of 1μW at a modulation rate of ~ 5 MHz, giving an energy of 200 fJ/bit. This power could be reduced very substantially if the p-i-n region were defined at submicron length scale around the quantum dot, which should lower the capacitance below 1 fF[28]. The quantum dot could be shifted through the cavity with a voltage below 100 mV [20]. We therefore expect that switching powers below $CV^2 < 0.01$ fJ/bit may be achieved for the QD-cavity system; the actual device power consumption would then likely be dominated by losses in the external circuitry.

#114379 - $15.00 USD Received 16 Jul 2009; revised 21 Sep 2009; accepted 24 Sep 2009; published 1 Oct 2009

4. Conclusions

In conclusion, we have demonstrated optical modulation in a strongly coupled quantum dot - cavity system realized in a p-i-n junction. When the field in the junction is controlled by optical injection of carriers, we find that the QD response time is limited by the 13-ns turn-on time of the tuning laser (a slower relaxation time currently limits the modulation frequency to ~ 5 MHz). We estimate a low switching energy of ~ 200 fJ. In future designs, the electric field could be controlled by electrical contacts to the p-i-n diode; this has been already been accomplished in single cavities[19, 20] and waveguide-integrated nanocavities [21], and has been shown in photonic crystal waveguides at a bit rate exceeding 1 Gbit/s[31]. The QD may also be shifted by a laterally applied electric field across a capacitor [32]. Using submicron wide contacts, electrical control of the p-i-n junction may be very fast, with an estimated RC time on the picosecond scale and energy-per-bit below 1 fJ. Our demonstration of optical modulation via a single quantum dot demonstrates the potential of solid-state cavity quantum electrodynamic systems for high-speed, low-power classical information processing.

Acknowledgments

We thank David A.B. Miller for helpful discussions. Financial support was provided by the DARPA Young Faculty Award, the Office of Naval Research (PECASE and ONR Young Investigator awards), the National Science Foundation, and the Army Research Office. A.M. was supported by the SGF (Texas Instruments Fellow). Work was performed in part at the Stanford Nanofabrication Facility of NNIN supported by the National Science Foundation.

#114379 - $15.00 USD Received 16 Jul 2009; revised 21 Sep 2009; accepted 24 Sep 2009; published 1 Oct 2009